Bispectra of a tropical coupled ocean–atmosphere system

M. Biswas, A. Chandrasekar and
B. N. Goswami*

Department of Physics and Meteorology, Indian Institute of Technology, Kharagpur 721 302, India
*Centre for Atmospheric Sciences, Indian Institute of Science, Bangalore 560 012, India

It has recently been proposed that the broad spectrum of interannual variability in the tropics with a peak around four years results from an interaction between the linear low-frequency oscillatory mode of the coupled system and the nonlinear higher-frequency modes of the system. In this study we determine the bispectrum of the conceptual model consisting of a nonlinear low-order model coupled to a linear oscillator for various values of the coupling constants.

IT has been well-established that the tropical ocean and the atmosphere interact strongly on time scales larger than a season and that the El Nino and Southern Oscillation (ENSO), an irregularly fluctuating interannual phenomenon, is a result of such interactions between the atmosphere and the ocean. For time scales in which the atmosphere cannot be considered in isolation, say time scales of the order of a season or longer, one must consider the tropical coupled ocean–atmosphere system. Only a few studies[1-3] have attempted to make a quantitative estimate of the predictability of the coupled ocean–atmosphere system. Goswami and Shukla[1] showed that the growth of small errors in the coupled

system is governed by two time scales. The fast time scale has an error-doubling time of about 5 months while the slow time scale has an error-doubling time of about 15 months. The slow time scale appears to arise as a result of the dominant four-year cycle of the system while the fast time scale appears to arise due to the aperiodicity of the system.

In general, aperiodicity may be attributed to nonlinear interaction between more than one mode (or degrees of freedom) of the system. Early instability analysis[4] shows that the tropical coupled ocean–atmosphere system possesses an unstable coupled low-frequency mode having a period of 26 months and an e-folding time of 5 months. Recent studies[5] have shown that the convergence feedback mechanism included in the parameterization of atmospheric heating introduced some higher-frequency intraseasonal unstable modes. The existence of more than one unstable mode can lead naturally to nonlinear interaction between them and thereby explain the existence of the aperiodicity. One of the efficient means of studying the existence of nonlinear interaction between different modes is by the determination of the bispectrum. For a normal random process the third moments are zero. The bispectrum is a decomposition in the frequency domain of the third moments and thus provides information on the nonlinear characteristics.

Krishnamurthy et al.[6] have recently proposed a conceptual model for the aperiodicity of the interannual variability of the tropics. The model consists of a nonlinear system (the Lorenz model[7]) coupled to a linear oscillator. The nonlinear system represents some aspects of the general circulation of the atmosphere and the equations are the same as those of Lorenz[7]. The linear part represents the dominant four-year oscillation of the

Table 1. The ten largest real bispectral values along with their periods (dim) for $\alpha = \beta = 0$. The standard deviations of our estimates of the above bispectral values are given in brackets m, w and y refer to months, weeks and years

X	0 02233; 7 5m, 6 67m (0 00002)	0 0156, 7.5m, 6m (0 00003)	0 0099, 7 5m, 5 45m (0.00004)	0 0055, 7 5m, 5m (0 00005)
X	0 0027, 7.5m, 4.62m (0.00002)	0 0011, 7 5m, 4 28m (0 000007)	0 0007, 6 67m, 4w (0 00001)	0 0006, 6 67m, 4 06w (0.00001)
X	0 0006, 6 67m, 1m (0 00001)	0 0005, 6 67m, 1 02m (0 00001)		
Y	0 0084, 7 5m, 2 39w (0.00065)	0 0077; 7 5m, 2 16w (0 00076)	0 0075, 7 5m, 2 1w (0.00098)	0 0073, 7 5m, 2.36w (0.00068)
Y	0 0072, 7.5m, 2 08w (0.00094)	0 0068; 7.5m, 2.34w (0 00069)	0 0068, 7 5m, 2 28w (0 00064)	0 0067, 7 5m, 2 2w (0.00060)
Y	0 0067, 7.5m, 2 24w (0 00061)	0 0067; 7 5m, 2 26w (0.00064)		
Z	0 0062; 2 39w, 4 26w (0 0002)	0 0062, 2 39w, 3 21w (0.00022)		0 006, 2 39w, 4 64w (0 00027)
Z	0 006; 2.39w, 4 7w (0 0003)	0 0059, 2 39w, 3w (0 00027)	0.0058, 2.39w, 2 98w (0 00028)	0 0055, 4 26w, 2 36w (0 00019)
Z	0 0054, 2.39w, 3 66w (0 00062)	0 0054, 2 39w, 3 42w (0 00025)		0 0054, 4 26w, 2 3w (0 00026)

Table 2. The ten largest imaginary part of the bispectral values along with their periods (dim) for $\alpha = \beta = 0$. The standard deviations of our estimates are also given in brackets. m, w and y refer to months, weeks and years

X	0 0005; 7 5m, 6 67m (0 00002)	0.0004; 7 5m, 6m (0 00003)	0 0003, 7.5m, 5 45m (0 00004)	0 0002, 2w, 3 94w (0.00011)
X	0 0002, 2w, 1m (0 00006)	0 0002, 2w, 4 26w (0 00007)	0 0002, 2w, 4w (0 00009)	0 0002, 2w, 4 73w (0.00004)
X	0 0002, 7 5m, 5m (0.00005)	0.0002, 3 94w, 3 66w (0 00007)		
Y	0 0081, 1 81m, 2 09w (0.00092)	0 0079, 1 81m, 2 11w (0 00094)	0 0078, 1 81m, 2 08w (0 00094)	
Y	0.0077, 1 8m, 2 13w (0 00093)	0 0076, 1 8m, 2.14w (0.00092)	0 0074, 1 8m, 2 22w (0 00086)	0 0074, 2 4w, 2 4w (0 00087)
Y	0 0074, 1 81m, 2 24w (0 00086)	0 0074, 1 81m, 2.28w (0 00090)	0 0074, 1 81m, 2 26w (0 00090)	
Z	0.0053, 2 39w, 4 64w (0 00027)	0.0052, 2 39w, 3w (0 00027)	0 0051, 2 39w, 3.21w (0 00022)	0 0049, 3w, 2 22w (0 00026)
Z	0 0049, 2 39w, 4 26w (0 00020)	0 0049, 3w, 2 24w (0 00026)	0.0048, 2 39w, 5 09w (0 00038)	
Z	0 0048, 2 39w, 2 86w (0 00037)	0 0047, 2 22w, 4 64w (0 00026)	0.0047; 3.02w, 2 2w (0 00025)	

coupled system arising due to unstable air–sea interactions in the tropics and reflection of Rossby waves from the western boundary[8]. Due to the very large horizontal scale involved, the equatorial Rossby number for this phenomenon is small and hence may be considered linear.

The equations of the coupled system may be written as[6]

$$\dot{X} = - Y^2 - Z^2 - aX + aF, \tag{1}$$

$$\dot{Y} = XY - bXZ - cY + G + \alpha P, \tag{2}$$

$$\dot{Z} = bXY + XZ - cZ + \alpha Q, \tag{3}$$

$$\dot{P} = -\omega Q - \beta Y, \tag{4}$$

$$\dot{Q} = \omega P - \beta Z, \tag{5}$$

where ω is the frequency of the low-frequency oscillator with a period of four years, P and Q are the amplitudes of the sine and the cosine phases of the oscillation and α and β are the coupling strengths. Equations (1)–(3) represent the high-frequency component while equations (4) and (5) represent the low-frequency component. The typical period of oscillation of the high-frequency coupled modes is in the intraseasonal range. In order that the nonlinear system (1)–(3) contain these intrinsic scales of the coupled system, we have rescaled Lorenz's equations by a factor c as (original variables denoted by primes)

$$t = t'c; \quad X = cX'; \quad Y = cY'; \quad Z = cZ';$$

$$a = a'c; \quad b = b'; \quad F = cF'; \quad G = c^2 G'$$

According to Lorenz, X may be interpreted as a zonally averaged field while Y and Z may be interpreted as amplitudes of the two wave components. F is interpreted as external zonally symmetric forcing (e.g. solar forcings) while G is the zonally asymmetric forcing (e.g. land–ocean contrast). We have used $c = 0.5$ and have retained the same values of the unscaled coefficients a' and b' as used by Lorenz, namely $a' = 0.25$ and $b' = 4$.

The time series was obtained by integrating the system of equations (1)–(5) for a period of 275 years. The first 50 years of data were discarded in order to eliminate transients. Data values with a sampling period of one week were stored. A record consisted of 260 data points, i.e a duration of 5 years. This yielded 45 nonoverlapping records for the entire 225 years data set. The bispectra were obtained for X, Y, Z, P and Q for the uncoupled case ($\alpha = \beta = 0$) and the coupled case ($\alpha = \beta = 0.1$). Also the same was obtained for cases ($\alpha = 0$, $\beta = 0.1$) and ($\alpha = 0.1$, $\beta = 0$). The forcings for the time series had an annual cycle in F ($F = 7.0 + 2.0 \cos 2\pi t/\tau$, where τ is one year) and a constant G ($G = 0.125$).

The procedure used to compute the bispectra was the same as employed by Lii et al.[9] and is as follows:

(i) After removing the mean of each record a cosine taper was applied. Each record was then Fourier-transformed to give 131 Fourier coefficients, $F(\lambda_k)$, where $\lambda_k = 0.1/n\ \delta t, 2/n\ \delta t, \ldots, 130/n\ \delta t$, where $n = 260$ and $\delta t = 1$ week $= 1.3846$ (dimensionless), i.e. we computed $F(\lambda_k)$, $k = 0, 1, 2, \ldots, n-1$; $n = 260$. Note that by symmetry we need to compute $F(\lambda_k)$ for $k = 0, 1, \ldots, 130$.

(ii) The bispectrum estimate

$$b(\lambda_k, \lambda_l) = (2\pi)^{-2}\ n^{-1}\ F(\lambda_k)\ F(\lambda_l)\ F^*(\lambda_k + \lambda_l),$$

$$k = l = 0, 1, \ldots, 130,\ (k + l) = 1 - 131$$

was computed for each record.

(iii) To reduce the variance we averaged at each (λ_k, λ_l) within a square neighbourhood 17×17, i.e. for the mth record

$$\bar{b}_m(\lambda_k, \lambda_l) = \frac{1}{289} \sum_{i=k-8}^{k+8} \sum_{j=l-8}^{l+8} b(\lambda_i, \lambda_j).$$

(iv) To reduce the variance further, we averaged 45 records to get an estimate

$$\bar{\bar{b}}_1(\lambda_k, \lambda_l) = \frac{1}{45} \sum_{m=1}^{45} \bar{b}_m(\lambda_k, \lambda_l).$$

We also computed the variance of the estimates as follows.

(v) Repeat steps (i)–(iv) in the computation of the bispectrum estimates for each mth record to get $\bar{b}_m(\lambda_k, \lambda_l)$.

(vi) Compute

$$\mathrm{Var}\,(\lambda_k, \lambda_l) = \frac{1}{45} \sum_{m=1}^{45} [\mathrm{Re}\ \bar{b}_m(\lambda_k, \lambda_l) - \mathrm{Re}\ \bar{\bar{b}}_1(\lambda_k, \lambda_l)]^2$$

and the corresponding variance for the imaginary part.

(vii) Compute $\mathrm{SD}(\lambda_k, \lambda_l) = [(1/45)\ \mathrm{Var}(\lambda_k, \lambda_l)]^{1/2}$ for both the real and imaginary parts. This gives the standard deviation of our estimates. The bispectral density can be obtained by dividing the bispectrum by the square of the frequency interval. The bispectrum values when multiplied by a factor of 129,600 would yield the bispectrum density. Since $\bar{\bar{b}}_1 (\lambda_k, \lambda_l)$ is complex, it is convenient to express its real and imaginary parts in normalized polar form to obtain the bicoherence

$$R^2(\lambda_k, \lambda_l) = \frac{(45)^3\ |\bar{\bar{b}}_1(\lambda_k, \lambda_l)|^2}{\displaystyle\sum_{m=1}^{45} |F(\lambda_k)|^2 \sum_{m=1}^{45} |F(\lambda_l)|^2 \sum_{m=1}^{45} |F(\lambda_k + \lambda_l)|^2}$$

and the phase

$$\phi(\lambda_k, \lambda_l) = \tan^{-1} \frac{\mathrm{Im}\{\bar{\bar{b}}_1(\lambda_k, \lambda_l)\}}{\mathrm{Re}\{\bar{\bar{b}}_1(\lambda_k, \lambda_l)\}}.$$

There are situations in practice where, because of interaction between two harmonic components of a process, there is contribution to the power at their sum and/or difference frequencies. Such a phenomenon, which is due to quadratic nonlinearities, gives rise to certain phase relations called quadratic phase coupling. It turns out that the power spectrum cannot provide for detection and quantification of quadratic phase coupling and one has to take recourse to the bispectrum. The physical significance of the power spectrum and the bispectrum is that while the former represents the contribution to the mean product of two Fourier components whose frequencies are the same, the latter represents the contribution to the mean product of three Fourier components, where one frequency equals the sum of the other two. The above physical significance becomes apparent when expressed in terms of the components $dZ(\omega)$ of the Fourier–Stieltjes representation of $X(k)$:

$$X(k) = \frac{1}{2\pi} \int_{-\infty}^{\infty} e^{j\omega k}\ dZ(\omega) \text{ for all } k,$$

where

$$E\{dZ(\omega)\} = 0,$$

$$E\{dZ(\omega_1)\ dZ^*(\omega_2)\} = \begin{cases} 0 & \text{for } \omega_1 \neq \omega_2, \\ 2\pi\ P(\omega)\ d\omega & \text{for } \omega_1 = \omega_2 = \omega, \end{cases}$$

Table 3. The ten largest real parts of the bispectrum along with their periods (dim) for $\alpha = \beta = 0$ 1. The standard deviations of our estimates are also given in brackets. m, w and y refer to months, weeks and years

X	0 0207. 7 5m, 6 67m (0 00013)	0 0146, 7 5m, 6m (0 00018)	0 0095, 7.5m, 5 45m (0 00025)	0 0056, 7 5m, 5m (0 00031)
X	0 0026, 7 5m, 4 62m (0 00009)	0 0021, 6 67m, 5 31w (0 00008)		0 0021, 6 67m, 5 42w (0 00008)
X	0 0021; 6 67m, 5 1w (0 00007)	0 0021; 6 67m, 5 2w (0 00007)		0 0021; 6 67m, 5w (0 00007)
Y	0 0079, 6 67m, 2 1w (0 00172)	0 0078, 6 67m, 2w (0 00139)	0 0076, 6 67m, 2 1w (0 0019)	0 0074, 6 67m, 2 14w (0 00153)
Y	0 0074, 6 67m, 2.02w (0 00176)	0 0073, 6 67m, 2 28w (0 00103)		0 0072, 6 67m, 2 13w (0.0016)
Y	0 0072, 6 67m, 2 24w (0 00144)	0.0072, 6m, 2 09w (0 00141)		0 0071, 6 67m, 2 3w (0 00097)
Z	0 0042; 2 24w, 6 67m (0 00087)	0 0041, 2 26w, 6 67m (0 00088)		0 0038, 4 91w, 2 3w (0 00056)
Z	0 0037; 2 32w, 4 91w (0 00059)	0 0036, 2 05w, 2w (0 00075)	0.0036, 2 02w, 2 05w (0 00094)	0.0036, 5w, 2 3w (0 00050)
Z	0 0035; 2 02w, 2 02w (0 00115)	0 0035, 5w, 2 32w (0 00053)		0 0035; 2 36w, 4 91w (0.00070)
P	0 03299; 6 67m, 7.5m (0 00338)	0 02697, 6m, 7 5m (0 00328)	0 01714, 5.45m, 7 5m (0 00282)	0 00943; 7.5m, 5m (0 0029)
P	0 00454. 4 62m, 7.5m (0 00106)	0 00215; 4 28m, 7 5m (0 00030)		0 00123; 4 62m, 6m (0 00014)
P	0 00116; 4 62m, 6 67m (0 00025)	0 00113; 4 62m, 5 45m (0 00014)		0 00105, 4m, 7 5m (0 00016)
Q	0 00497; 7 5m, 7 5m (0 00187)	0 00497, 8 57m, 8 57m (0 00189)		0 00497, 8 57m, 10m (0 00189)
Q	0 00497, 8 57m, 12m (0 00189)	0 00497, 8 57m, 15m (0 00189)		0 00497, 8 57m, 20m (0.00189)
Q	0.00497; 8 57m, 30m (0 00189)	0 00497, 8 57m, 5y (0 00189)	0 00497; 10m, 10m (0 00187)	0 00497; 10m, 12m (0 00189)

$$E\{dZ(\omega_1)\ dZ(\omega_2)\ dZ^*(\omega_3)\} =$$

$$\begin{cases} 0 & \text{for } \omega_1 + \omega_2 \neq \omega_3, \\ b(\omega_1, \omega_2)^2\ d\omega_1\ d\omega_2 & \text{for } \omega_1 + \omega_2 = \omega_3, \end{cases}$$

where $P(\omega)$ and $b(\omega_1, \omega_2)$ refer to the power spectrum and bispectrum and $E\{\ \}$ is the expectation.

Tables 1 and 2 provide the values of the real and imaginary parts of the bispectrum values of X, Y and Z for the uncoupled case $(\alpha = \beta = 0)$. The largest 10 bispectrum values (not in absolute magnitude) along with the corresponding periods (dimensional) are given. The standard deviation of our estimates for the above bispectral values are also provided within brackets just below the bispectral values. It is found that the bispectra for P and Q for the uncoupled case are very small (of the order of 10^{-8}) and therefore not presented here. It is obvious that with $\beta = 0$ the components of low-frequency oscillation (P and Q) should exhibit no nonlinearity and, consequently, should have zero bispectrum. As seen in Tables 1 and 2 the standard deviations of our estimates are very much smaller compared to the bispectral values. The real part of the bispectrum for X has nonlinear interaction between the mode with a time scale of 7.5

months and modes with a time scale of 4–6 months. There also seems to be some interaction between modes having time scales of 6 and 1 month. We also find that the imaginary part of the bispectral values for X is much smaller in magnitude compared to the real part. The imaginary part of the bispectral values for X has interaction between the mode having a time scale of 7.5 months with that having a time scale of 5–6 months. In addition to the above, we find that the mode with a time scale of 4 weeks interacts with that having a time scale of 2 weeks. The bispectrum values for Y, especially the real part, seem smaller compared to those of X. However, we find that for the real part of the bispectrum for Y the mode with a time scale of 7.5 months has strong interaction with modes having a time scale of around 2 weeks. The imaginary part of the bispectrum for Y, unlike that of X, is comparable in magnitude to the real part of the spectrum and has interaction between modes having time scales of 2 months and 2 weeks. The bispectrum values for Z are comparable to those of Y. For the real part of the bispectrum for Z the mode with a time scale of 2 weeks seems to interact with modes having time scales of 3–4 weeks. The imaginary part of the bispectrum values for Z has interaction between modes

Table 4. The ten largest imaginary parts of the bispectral value along with their periods (dim) for $\alpha = \beta = 0\ 1$
The standard deviations of our estimates are given in brackets

λ	0 00064, 7 5m, 5m (0 00031)	0 00063, 7 5m, 6 67m (0 00013)	0 00059, 7 5m, 5.45m (0 00025)	0 00055, 7 5m, 6m (0 00018)
X	0 0004, 4 91w, 4 91w (0 00005)	0 00037, 4 81w, 4 91w (0 00005)		0 00035, 4 19w, 4 19w (0 00004)
X	0 00035, 4 81w, 4 81w (0 00005)	0 00034, 4 19w, 4 33w (0 00004)		0 00034, 4 33w, 4 13w (0.00004)
Y	0 0038, 2 09w, 2 09w (0 00093)	0 0036, 2 09w, 2 08w (0 00106)		0 0036, 5m, 2 09w (0 00122)
Y	0 0035, 2 08w, 2 08w (0 0015)	0 003, 2w, 5m (0 001089)	0 0031, 2 22w, 5m (0 001087)	0 0031; 2 4m, 2 09w (0 001305)
Y	0 0031, 5 45m, 2 09m (0 00129)	0 0031; 2 24w, 2 4w (0 00124)		0 003, 2.02w, 5m (0 00141)
Z	0 0039, 2 36w, 4 91w (0 0007)	0.0039, 2.34w, 6 05w (0 00061)		0 0039, 2.36w, 4 81w (0 00072)
Z	0 0038, 2 34w, 4 9w (0 00066)	0 0037, 2 36w, 6 05w (0 00062)		0 0037, 2 34w, 4 81w (0 00068)
Z	0 0037, 4 8w, 2 3w (0 00057)	0.0036, 2 36w, 5 5w (0 00069)	0 0036, 2 34w, 5 5w (0.00067)	0 0036, 2 3w, 6 05w (0 00056)
P	0 00903; 7 5m, 7 5m (0 02044)	0 00903; 8 57m, 8 57m (0 02067)		0 00903, 8 57m, 10m (0 02067)
P	0 00903; 8 57m, 12m (0 02067)	0 00903, 8 57m, 15m (0 02067)		0 00903, 8 57m, 20m (0 02067)
P	0 00903; 8 57m, 30m (0 02067)	0 00903; 8 57m, 5y (0 02067)	0 00903, 10m, 10m (0.02067)	0 00903, 10m, 12m (0 02067)
Q	0 0001; 6 67m, 6m (0 00006)	0 00006, 6m, 6m (0 00004)	0 00002, 6 67m, 5.45m (0 00004)	0 00001, 5 45m, 6m (0 00004)
Q	0 00001; 5m, 6m (0.000007)	0.000009; 4.62m, 7 5m (0 000a05)		0 000008, 3 33m, 7.5m (0 000005)
Q	0.000008, 5 45m, 5 45m (0 000009)	0 000008, 7.5m, 4m (0 00001)		0 000006, 2.3w, 7 5m (0 000004)

with a time scale of 2 weeks and modes having a time scale of 3–5 weeks.

For the coupled case ($\alpha = \beta = 0.1$), with G and F remaining the same, the bispectral coefficients were determined (Tables 3 and 4). One would expect that the introduction of coupling would result in the appearance of nonlinear interaction between various modes for P and Q. It is found that the real part of the bispectrum for P has interaction between the mode having a time scale of 7.5 months and modes having a time scale of 4–6 months. In addition to the above, we find that the mode with a time scale of 4 months interacts with the mode having a time scale of 5–6 months. The imaginary part of the bispectrum for P has values very much smaller than the standard deviation estimates and, consequently, is unreliable. The bispectrum estimates of Q for the coupled case have magnitudes very much smaller compared to P. The real part of the bispectrum for Q has interaction between the mode with a time scale 8 months and several modes of time scale between 10–60 months. The imaginary part of the bispectrum for Q has interaction between the mode with a time scale 6 months and modes with a time scale 5–6 months. The bispectrum for X for the coupled case is similar in magnitude to that for

the uncoupled case, except that for the real part of X the modes having a time scale of 6 months and 5 weeks are seen to interact. Also for the imaginary part of X for the coupled case the mode with a time scale of 4 weeks is found to interact with itself. This is at variance with the uncoupled case, where the mode with a time scale of 4 weeks interacted with that having a time scale of 2 weeks. For the imaginary part of the bispectrum for Y for the coupled case, an additional nonlinear interaction between the mode having a time scale 5 months with that having a time scale of 2 weeks manifests itself. For the real part of the bispectrum for Z for the coupled case, an additional interaction between the mode having a time scale of 2 weeks with that having a time scale of 6 months manifests itself.

A better way of representing the bispectral values and the estimates of the standard deviation was thought of as follows. The real and imaginary parts of the bispectral values will be depicted by horizontal and vertical arrows, with the length of the arrow indicating the magnitude of the bispectra. The corresponding standard deviation estimates of the above bispectral values will be depicted by error bars which will be vertical for the real part and horizontal for the imaginary part. The
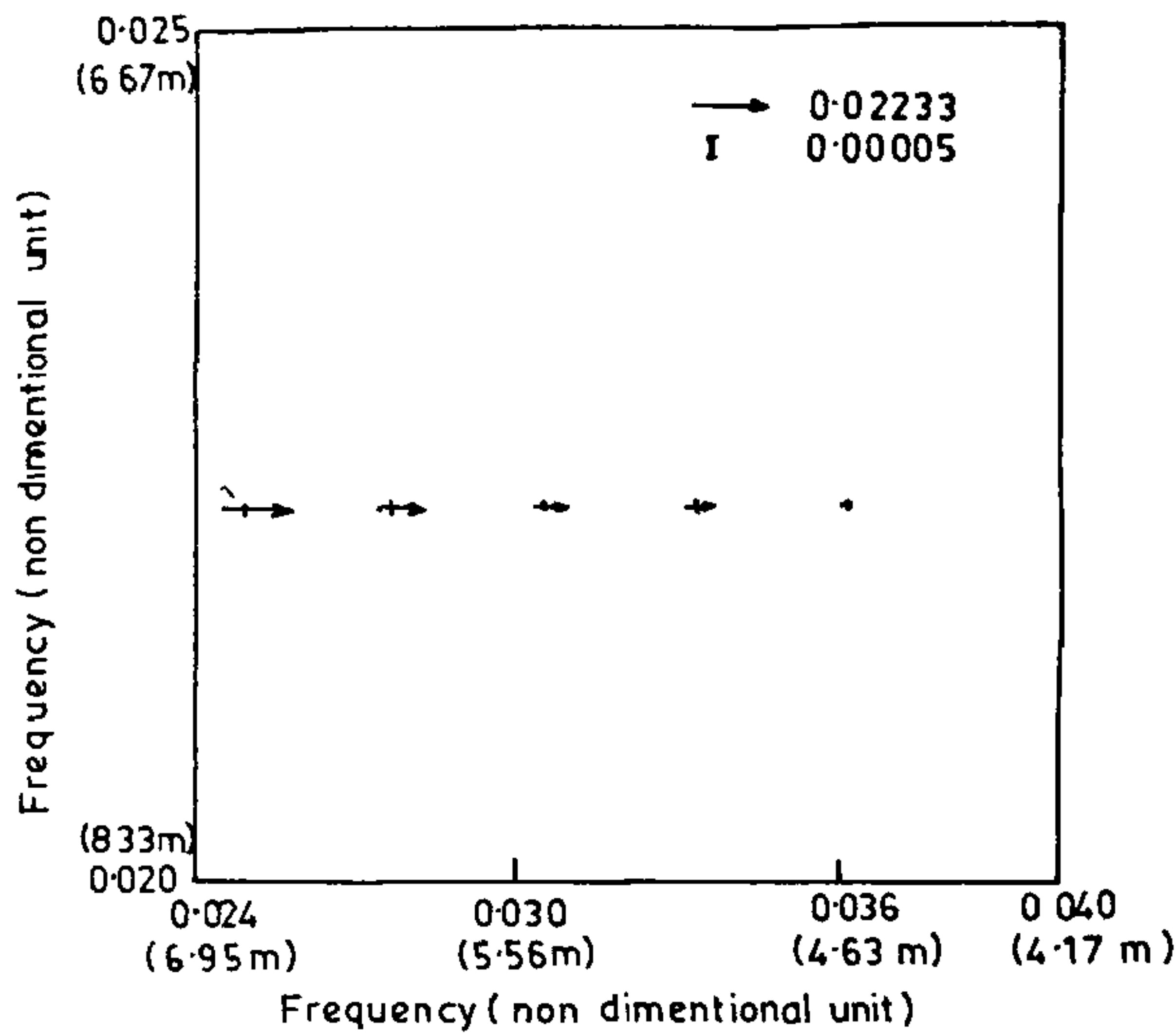
Figure 1. The real and imaginary parts of the bispectral values along with the standard deviation estimates for X for the uncoupled case $(\alpha = \beta = 0)$ and $G = 0.125$
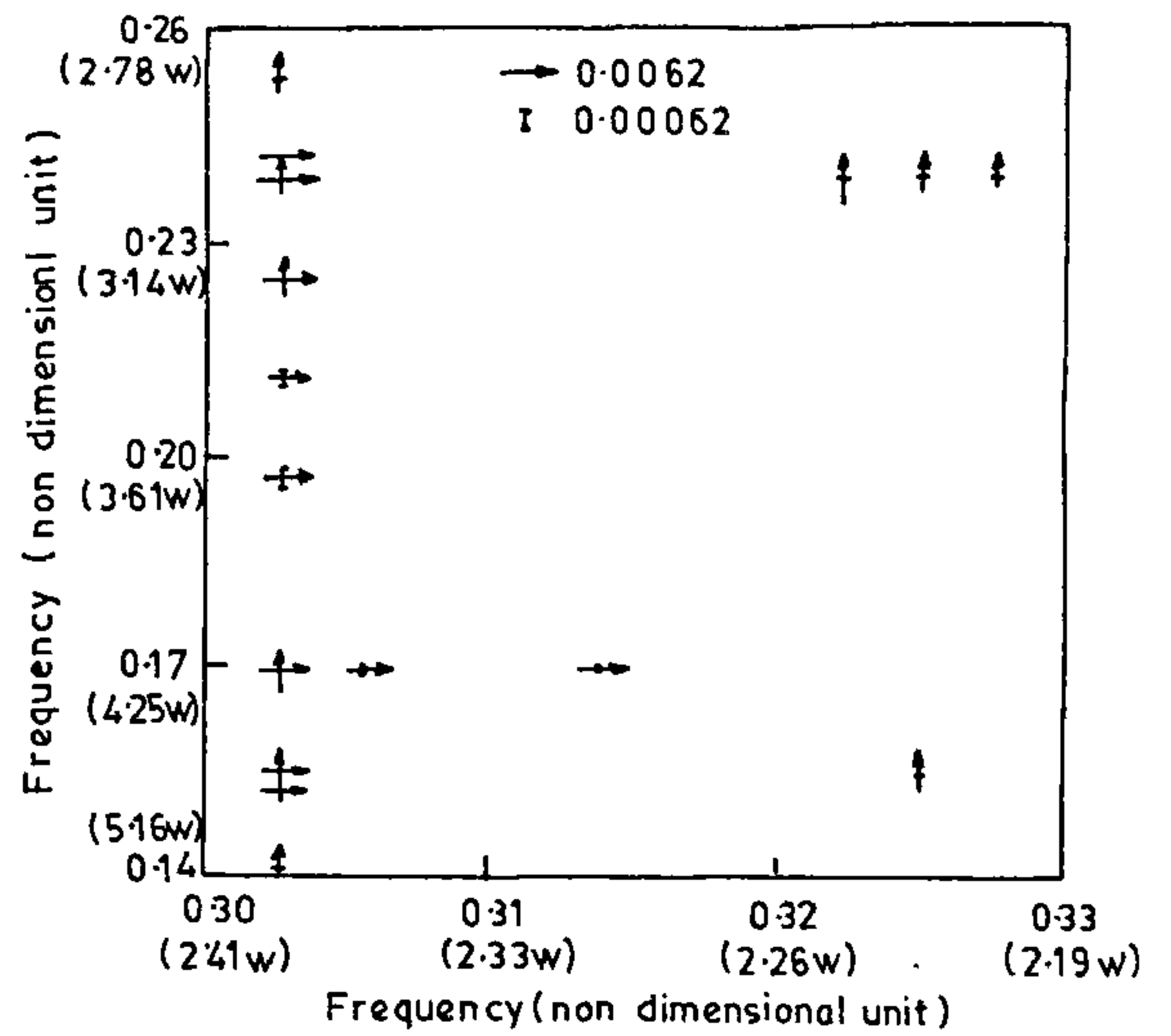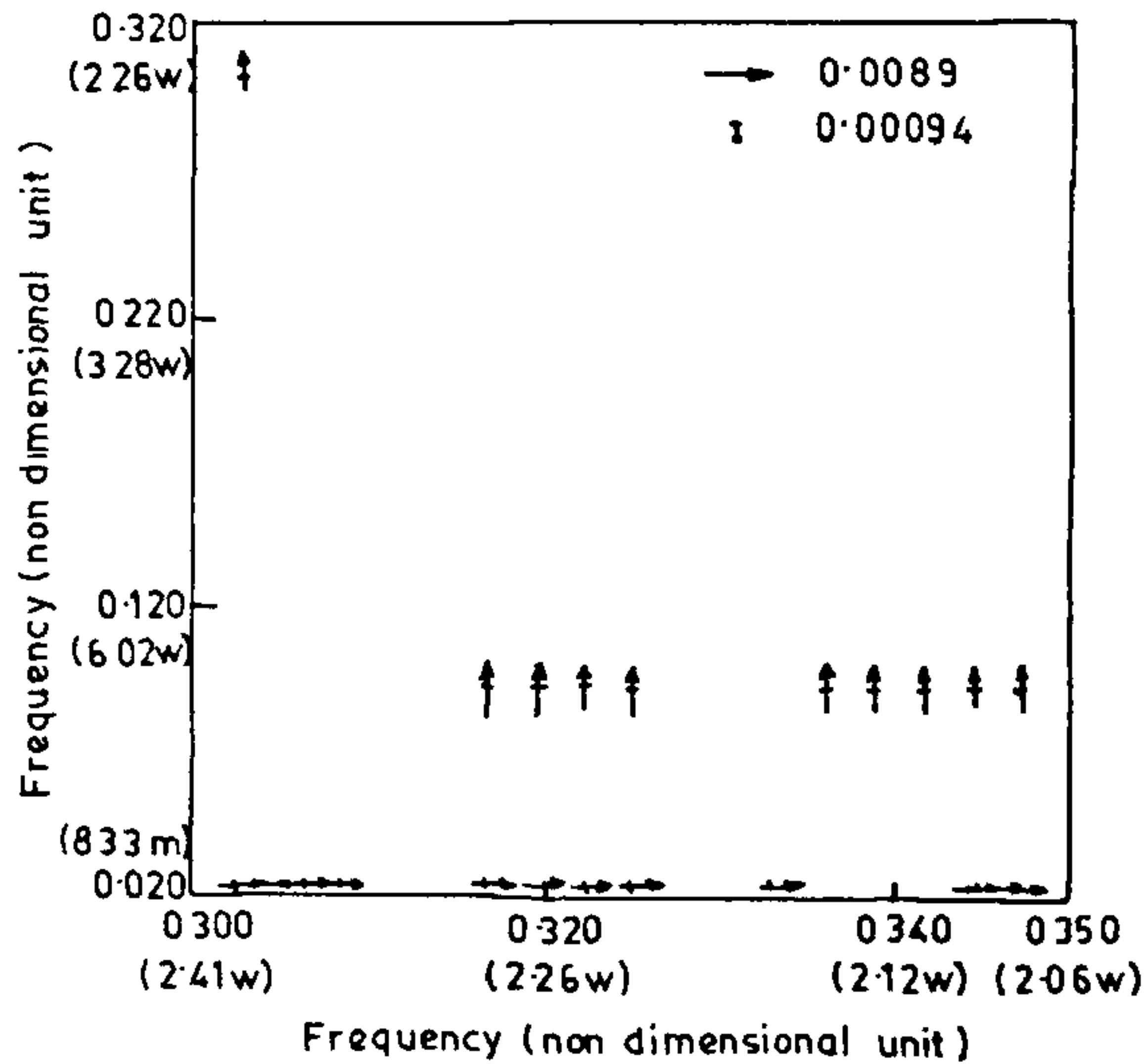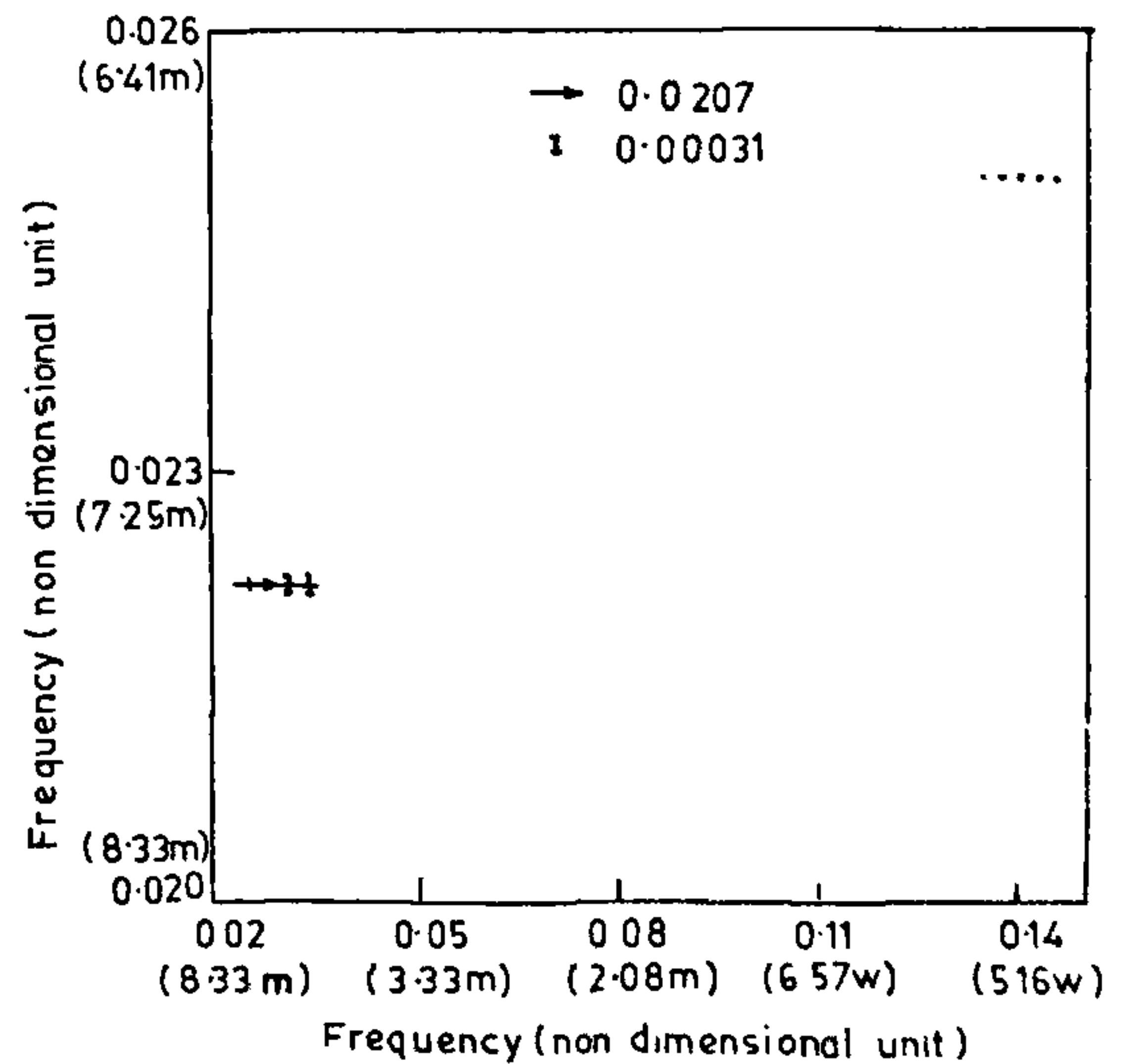

Figure 3. The real and imaginary parts of the bispectral values along with the standard deviation estimates for Z for the uncoupled case $(\alpha = \beta = 0)$ and $G = 0.125$

Figure 2. The real and imaginary parts of the bispectral values along with the standard deviation estimates for Y for the uncoupled case $(\alpha = \beta = 0)$ and $G = 0.125$
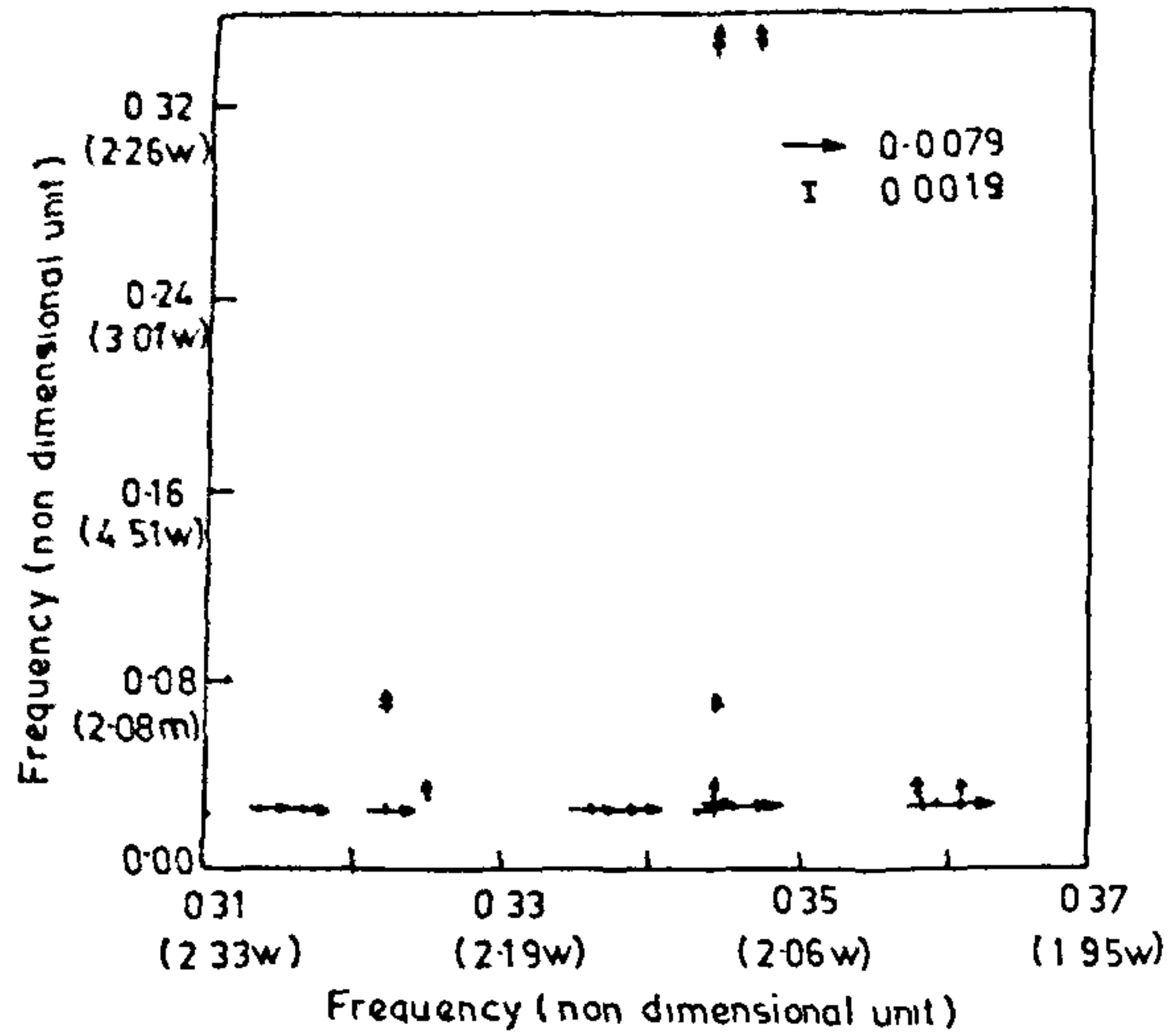

Figure 4. The real and imaginary parts of the bispectral values along with the standard deviation estimates for X for the coupled case $(\alpha = \beta = 0.1)$ and $G = 0.125$

magnitude of the estimates of the standard deviation will be indicated by the length of the bar. The position of the bar coincides with the respective frequency (the corresponding value of the dimensional period is also provided within brackets) and is always found to be in the mid-point of the arrow. Figures 1–3 depict the bispectral values and the estimates of the standard deviation for

the uncoupled case $(\alpha = \beta = 0)$ for X, Y and Z, while Figures 4–8 depict the same for the coupled case $(\alpha = \beta = 0.1)$ for X, Y, Z, P and Q.

We find that the inclusion of the coupling strengths has led to the appearance of additional modes of nonlinear interaction in Y, Z, P and Q having time scales of the order of 4–8 months. The bispectrum for X is more or

Figure 5. The real and imaginary parts of the bispectral values along with the standard deviation estimates for Y for the coupled case ($\alpha = \beta = 0.1$) and $G = 0.125$
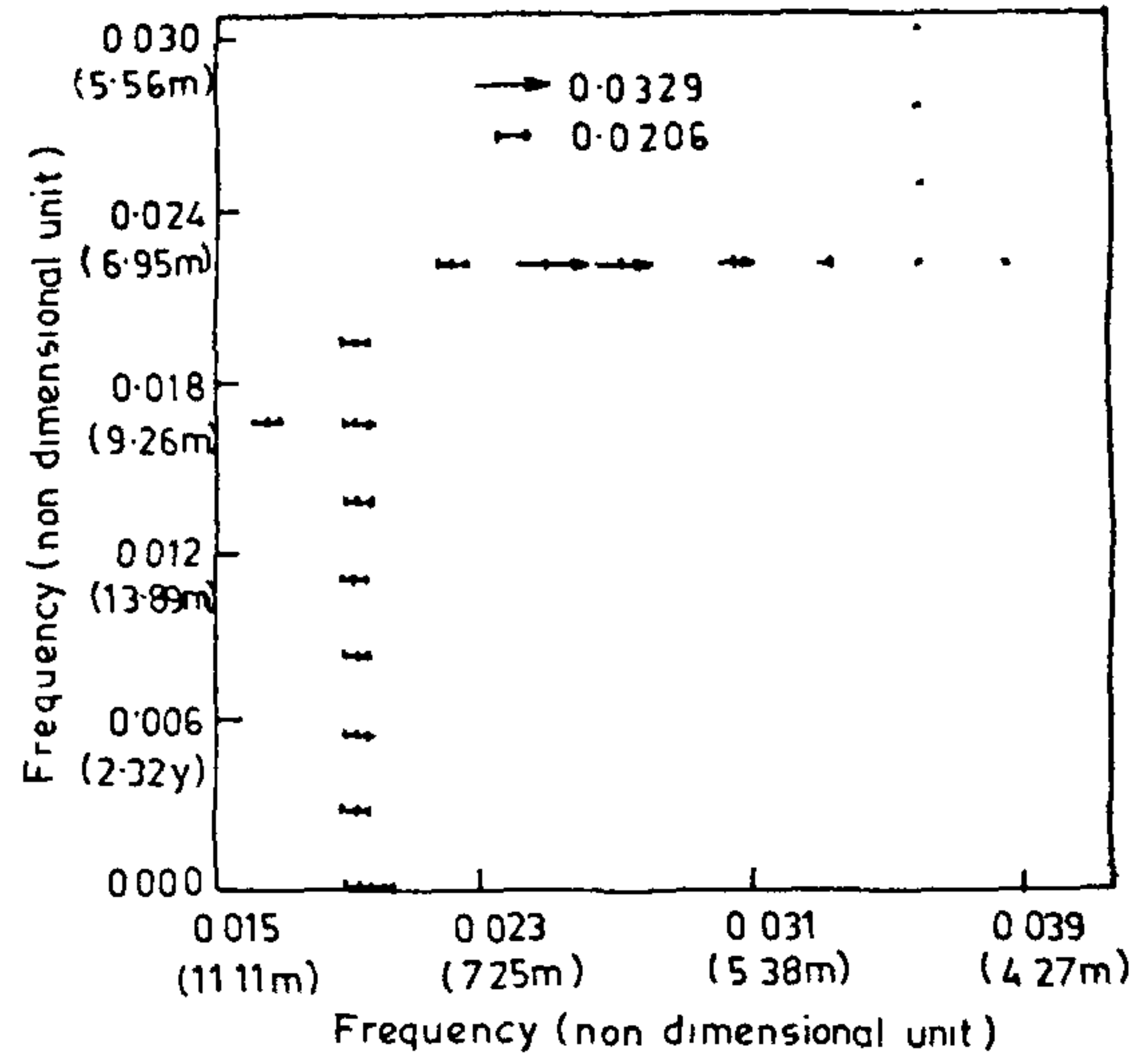

Figure 7. The real and imaginary parts of the bispectral values along with the standard deviation estimates for P for the coupled case ($\alpha = \beta = 0.1$) and $G = 0.125$
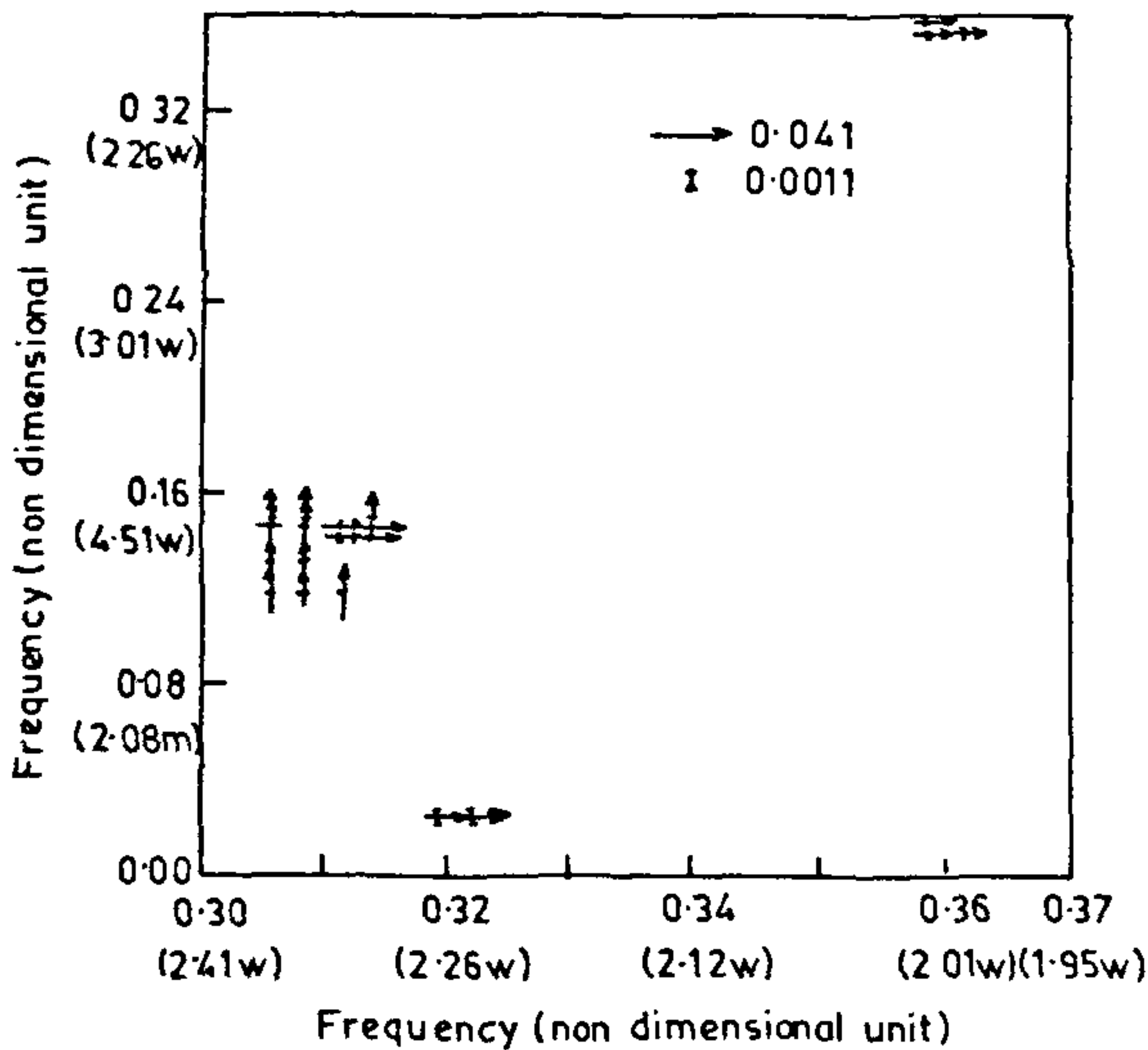

Figure 6. The real and imaginary parts of the bispectral values along with the standard deviation estimates for Z for the coupled case ($\alpha = \beta = 0.1$) and $G = 0.125$.
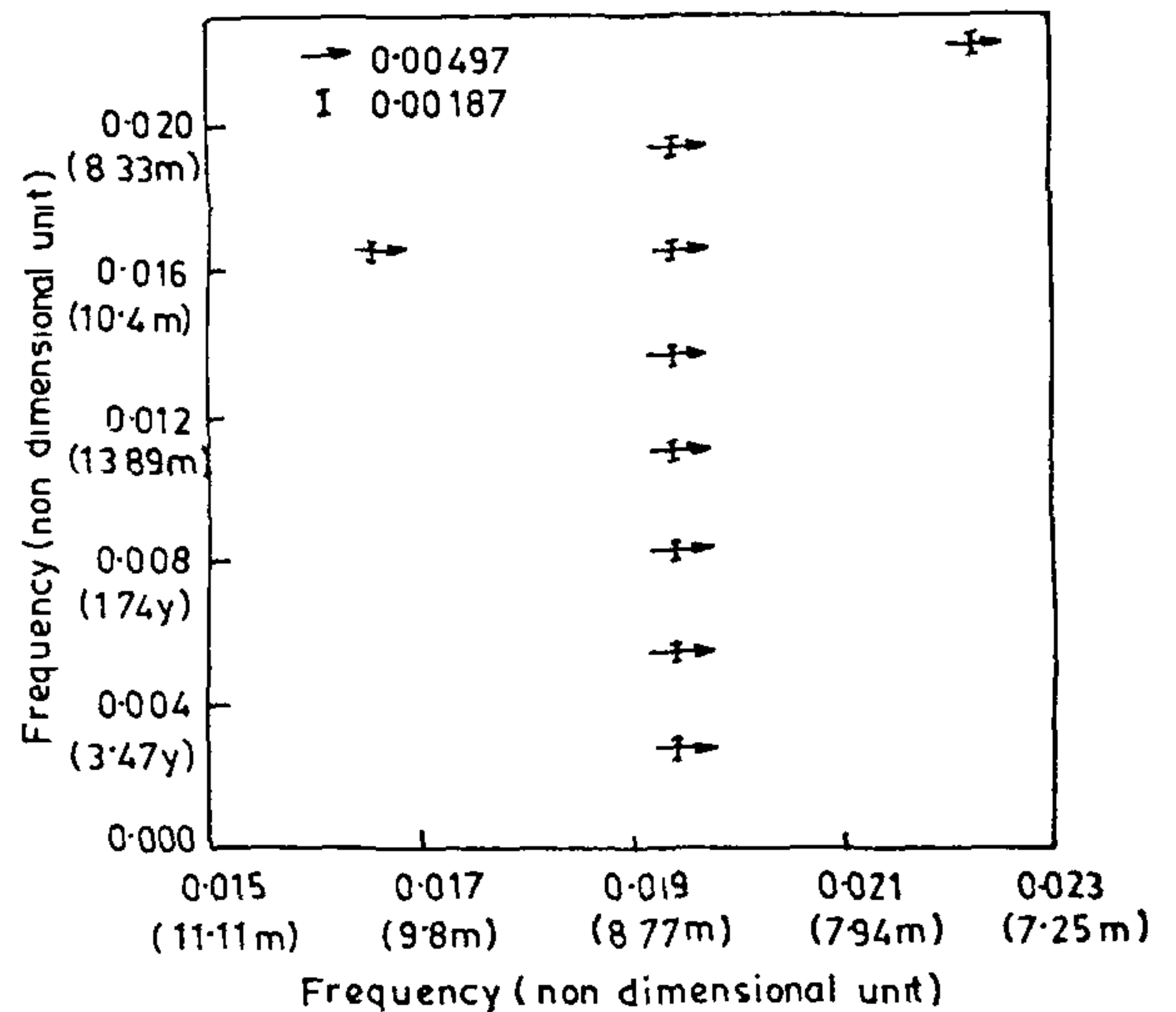

Figure 8. The real and imaginary parts of the bispectral values along with the standard deviation estimates for Q for the coupled case ($\alpha = \beta = 0.1$) and $G = 0.125$

less unaffected by coupling. This seems reasonable as the coupling of the higher-frequency oscillation to the low-frequency oscillation is assumed to take place through the nonzonal components (Y, Z). It is pertinent to recall here that the unstable coupled mode found by Hirst[4] was profoundly modified by the convergence feedback mechanism[10] and that the period of the Hirst mode changed from 26 months to ~7–8 months for a wavelength of 10,000 km ($k = 0.15$) and for the strength

of convergent feedback $q_s = 0.95$. Also the periods of the gravest eastward and westward propagating additional modes arising due to the convective feedback mechanism were[10] of the order of 3–4 months for $q_s = 0.95$ and $k = 0.15$. This lends further credence to the fact that the above conceptual model does exhibit certain important features of the variability in the tropics. The similarity between the results of this study and

those of an earlier study[10] suggests that the conceptual model can indeed serve as a simple coupled ocean–atmosphere model with general ocean thermodynamics.

Krishnamurthy et al.[6] have earlier demonstrated that the aperiodicity in the interannual variability in the tropics is due to the interaction between the low-frequency mode and the nonlinear higher-frequency modes. In general, aperiodicity arises due to nonlinear interaction between more than one modes of the system. One way of studying the nonlinear interaction between different modes is through the determination of bispectrum. The bispectrum of the conceptual model for the coupled case ($\alpha = \beta = 0.1$) gave rise to additional modes with time scales very similar to those found in the earlier study of Selvarajan and Goswami[10], who employed a simple coupled ocean–atmosphere system with general ocean theromodynamics, in which the atmosphere heating is determined by sea surface temperature anomalies as well as the convergence feedback mechanism. This study further establishes the fact that the conceptual model does exhibit important characteristics of variability of the tropics.

1 Goswami, B N and Shukla, J, *J. Climate*, 1991, **4**, 3–21.
2 Bluementhal, M. B and Paul Bryant, *Phys. Rev*, 1991, **A43**, 2787–2806.
3 Latif, M and Flugel, J, *Geophys Res.*, 1991, **96**, 2661–2673
4 Hirst, A. C., *J. Atmos Sci*, 1986, **43**, 606–630.
5 Goswami, B N. and Selvarajan, S., *Geophys Res. Lett.*, 1991, **18**, 991–994
6 Krishnamurthy, V., Goswami, B N and Legnani, R., *Geophys. Res. Lett*, 1993, **20**, 435–438
7. Lorenz, E. N., *Tellus*, 1984, **A36**, 98–110
8 Suarez, M J. and Schopf, P. S, *J. Atmos Sci.*, 1988, **45**, 3283–3287
9. Lii, K S, Rosenblatt, M. and Van Atta, C. W, *J Fluid Mech*, 1976, **77**, 45–62.
10 Selvarajan, S and Goswami, B N, *Proc Indian Acad Sci. (Earth Planet Sci)*, 1992, **10**, 153–176